Luminescent heteroleptic copper(I) complexes with polydentate benzotriazolyl-based ligands

Valentina Ferraro[1] · Jesús Castro[2] · Lodovico Agostinis[3] · Marco Bortoluzzi[1,4]

Accepted: 31 March 2021

Abstract
Bis(benzotriazol-1-yl)phenylmethane $CHPh(btz)_2$ and tris(benzotriazol-1-yl)methane $CH(btz)_3$ were used as N-donor ligands to prepare luminescent heteroleptic copper(I) complexes. $[Cu\{CHPh(btz)_2\}(PPh_3)_2][BF_4]$ and $[Cu\{CHPh(btz)_2\}(DPEphos)][BF_4]$ (DPEphos = bis[(2-diphenylphosphino)phenyl] ether) were obtained from the corresponding borohydride complexes $[Cu(BH_4)(PPh_3)_2]$ and $[Cu(BH_4)(DPEphos)]$ and tetrafluoroboric acid. $[Cu\{CH(btz)_3\}(PPh_3)][BF_4]$ and $[Cu\{CH(btz)_3\}(P^iPr_3)][BF_4]$ were prepared from the acetonitrile complex $[Cu(NCCH_3)_4][BF_4]$. The complexes exhibited bright yellow or orange emissions upon excitation with near-UV and violet light. The photoluminescent properties were attributed to metal-to-ligand charge transfer transitions on the basis of experimental data and DFT calculations.

Introduction

Luminescent earth-abundant transition metal complexes are nowadays extremely appealing from a technological point of view as they can be used in advanced applications [1–4]. Copper(I) coordination compounds play a role of paramount importance in this field, because suitable triplet excited states can produce strong emissions with luminescence performances comparable to the commonly used iridium(III) and platinum(II) derivatives [5, 6]. Moreover, the possibility of harvesting also singlet excited states originates a peculiar feature in luminescent copper(I) complexes, called thermally activated delayed fluorescence (TADF), of huge interest for applications in organic light-emitting diodes (OLEDs) technology [7–9].

✉ Valentina Ferraro
valentina.ferraro@unive.it

1 Dipartimento di Scienze Molecolari e Nanosistemi, Università Ca' Foscari Venezia, Via Torino 155, Mestre (Ve) 30172, Italy

2 Departamento de Química Inorgánica, Universidade de Vigo, Edificio de Ciencias Experimentais, Vigo 36310, Galicia, Spain

3 Aimplas, Plastic Technology Center, Valencia Parc Tecnologic, Valencia Parc Tecnologic, C/Gustave Eiffel, 4, 46011 Valencia, Spain

4 Consorzio Interuniversitario Reattività Chimica e Catalisi (CIRCC), via Celso Ulpiani 27, 70126 Bari, Italy

The pivotal investigation of McMillin et al. on the 1,10-phenantroline skeleton allowed to point out several intriguing aspects of copper(I) luminescence [10]. Size, chemical nature and position of the substituents on the 1,10-phenantroline skeleton strongly influence the emission, originated from a metal-to-ligand charge transfer (MLCT) excited state [11–14]. In the case of heteroleptic complexes, the transition normally involves the highest occupied molecular orbital (HOMO), mainly constituted by the lone pair of the phosphine and the d orbitals of the metal centre, and the lowest unoccupied molecular orbital (LUMO), mostly localized on the π* orbitals of the N-donor ligands [15].

An alternative to the polypyridines mentioned above is the use of azoles as N-donor ligands. Benzimidazole was deeply investigated for the preparation of luminescent Cu(I) complexes [16–18]. On the contrary, besides being extremely versatile, benzotriazole was mostly considered as building block for organic synthesis [19, 20]. The use of benzotriazole and its derivatives in coordination chemistry was mostly limited to Cu(II) as metal centre [21], for instance with the isolation of bis(benzotriazol-1-yl)methane coordination polymers [22–24]. Poly(benzotriazol-1-yl) borates were successfully coordinated to Cu(I) [25], but less attention was devoted to the isoelectronic tris(benzotriazol-1-yl)methane $CH(btz)_3$, although this compound is known since the 1980s [26–30].

Our research group is currently focused on the synthesis and characterization of luminescent first row transition metal complexes [31–37]. We improved the synthesis of

bis(benzotriazol-1-yl)arylmethanes [38] and the same procedure was later extended to bis(indazol-1-yl)phenylmethane. This last species was used as chelating ligand for the preparation of an homoleptic luminescent Cu(I) complex [39]. Following the previously reported results, bis(benzotriazol-1-yl)phenylmethane and tris(benzotriazol-1-yl)methane were chosen as possible bi- and tridentate ligands for the preparation of new luminescent heteroleptic Cu(I) complexes.

Experimental section

Materials

Commercial solvents (Aldrich) were purified following reported procedures in order to be used inside the glove box [40]. The other reagents were Aldrich, TCI or Carlo Erba products and used as received. Triisopropylphosphine was used as 10% wt. solution in hexane and stored inside the glove box to avoid decomposition.

CuCl was synthesized according to literature procedures using sodium sulphite as reducing agent [41]. $[Cu(NCCH_3)_4][BF_4]$ was obtained from Cu_2O following a reported synthesis [42]. $[Cu(BH_4)(PPh_3)_2]$ was prepared on the basis of a literature method [43], while [Cu(BH4)(DPEphos)] (DPEphos = bis[(2-diphenylphosphino)phenyl] ether) was obtained starting from CuCl and DPEphos, using $NaBH_4$ as borohydride source. The ligand bis(benzotriazol-1-yl)phenylmethane $CHPh(btz)_2$ was prepared as previously reported by our research group from benzaldehyde, bis(benzotriazol-1-yl) methanone and catalytic amounts of anhydrous $CoCl_2$ [38]. Tris(benzotriazol-1-yl)methane $CH(btz)_3$ was obtained from benzotriazole, chloroform and sodium hydroxide following a procedure reported in literature [44]. Crystals of this compound suitable for X-ray diffraction were collected from the slow evaporation of dichloromethane solutions.

Instrumentation

The syntheses of the complexes starting from the acetonitrile precursor were carried out under inert atmosphere in a glove box (MBraun Labstar with MB 10 G gas purifier) filled with N_2 and equipped for inorganic syntheses. The other syntheses were performed using common Schlenk techniques.

Elemental analyses (C, H, N) were carried out using an Elementar Unicube microanalyser. Conductivity measurements in acetone were taken with a Radiometer Copenhagen CDM83 instrument. Melting point measurements were taken using a modified Falc 360 D apparatus equipped with a video recording device. TGA measurements were taken under N_2 atmosphere with a Q5000 instrument V3.17 Built 265. The heating rate was set at 20 °C min^{-1} from 30 °C up to 500 °C. IR spectra (KBr discs) were collected in the range of 4000–400 cm^{-1} using a PerkinElmer Spectrum One spectrophotometer. Monodimensional nuclear magnetic resonance (NMR) spectra were collected at variable temperature employing Bruker Avance 300 and Avance 400 instruments operating, respectively, at 300.13 MHz and 400.13 MHz of ^1H resonance. ^1H NMR spectra are referred to the partially non-deuterated fraction of the solvent, itself quoted to tetramethylsilane. ^{31}P $\{^1H\}$ NMR and ^{11}B NMR resonances are, respectively, referred to 85% H_3PO_4 in water and $BF_3{\cdot}Et_2O$ complex in $CDCl_3$. UV/Vis absorption spectra were collected for dichloromethane solutions using a PerkinElmer Lambda 40 spectrophotometer. Photoluminescence emission (PL) and excitation (PLE) measurements were taken at room temperature on solid samples using a Horiba Jobin Yvon Fluorolog-3 spectrofluorometer. A continuous wave Xe arc lamp was used as source selecting the excitation wavelength using a double Czerny–Turner monochromator. A single grating monochromator coupled to a photomultiplier tube was used as detection system for optical emission measurements. Excitation and emission spectra were corrected for the instrumental functions. Time-resolved analyses were performed using pulsed UV LED sources (Horiba SpectraLed). The photoluminescence quantum yields (ϕ) of the complexes (solid state, r.t.) were measured by means of a OceanOptics HR4000CG UV-NIR detector, fibre coupled to an integrating sphere connected to an OceanOptics LED source centred at 365 nm.

UV LEDs VCC VAOL-5EUV8T4, characterized by maximum of emission at 385 nm and luminous intensity of 100 mcd, were purchased from RS Components and connected to a Keithley 2400 Source Meter. The emission spectrum was registered between 400 and 1035 nm using an OceanOptics Flame T spectrophotometer paired with an optical fibre, an achromatic collimating lens and a long pass filter with cut-off wavelength of 395 nm.

Synthesis of the complexes

$[Cu\{CHPh(btz)_2\}(PPh_3)_2][BF_4]$ (**1**) and $[Cu\{CHPh(btz)_2\}$ (DPEphos)$][BF_4]$ (**2**) (DPEphos = bis[(2-diphenylphosphino)phenyl] ether) were obtained from the corresponding borohydride complexes (Scheme 1). In a typical preparation, $HBF_4{\cdot}Et_2O$ (0.4 mL, 3.0 mmol) was added to a dichloromethane solution (20 mL) of $CHPh(btz)_2$ (0.490 g, 1.5 mmol). After 5 min, the solvent was evaporated under reduced pressure and $[Cu(BH_4)(PPh_3)_2]$ or [Cu(BH4)(DPEphos)] (1.0 mmol) were added as solids. The reagents were put under inert atmosphere and cooled at −196 °C with a liquid nitrogen bath. Dichloromethane (20 mL) was then slowly added through a syringe, and the reaction mixture was allowed to slowly warm to room temperature. After stirring overnight, the solution was purified by filtration and the solvent was evaporated under reduced pressure. The addition

Scheme 1 Synthesis of the Cu(I) complexes

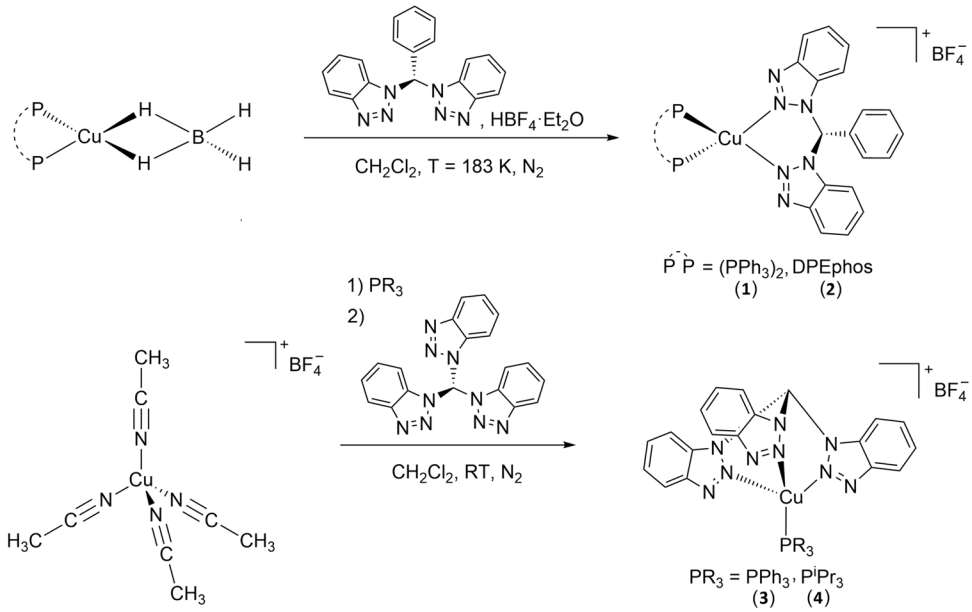

of diethyl ether (20 mL) caused the separation of a solid that was filtered, washed with 5 mL of diethyl ether and dried under vacuum. Yield of (**1**) 0.711 g (71%). Yield of (**2**) 0.761 g (75%).

[Cu{CH(btz)$_3$}(PPh$_3$)][BF$_4$] (**3**) and [Cu{CH(btz)$_3$}(P^{i}Pr$_3$)][BF$_4$] (**4**) were prepared from the acetonitrile complex [Cu(NCCH$_3$)$_4$][BF$_4$] (Scheme 1). The precursor (0.315 g, 1.5 mmol) was dissolved in 20 mL of dry dichloromethane, and a stoichiometric amount of the proper phosphine was added to the solution. The reaction mixture was stirred at room temperature for 4 h, then tris(benzotriazol-1-yl)methane (0.367 g, 1.0 mmol) was added and the solution was left overnight under stirring. The solvent was then evaporated under reduced pressure, and after adding 20 mL of diethyl ether, the solid obtained was filtered, washed with 5 mL of diethyl ether and dried under vacuum. Yield of (**3**) 0.616 g (79%). Yield of (**4**) 0.475 g (70%).

Poly(methyl methacrylate) samples (PMMA, M_w = 86,000 g mol^{-1}, TCI Chemicals) doped with the complexes were obtained from dichloromethane solutions. In a typical preparation, the proper complex (*ca.* 2 mg) was dissolved in a CH_2Cl_2 solution (0.5 mL) containing 50 mg of PMMA. The solution was allowed to dry at room temperature on the surface of a commercial LED.

Characterization of (**1**). Elemental analysis for $C_{55}H_{44}BCuF_4N_6P_2$, calcd: C, 66.0%, H, 4.4%, N, 8.4%. Found: C, 65.7%, H, 4.5%, N, 8.4%. M.p. (°C): 105 (dec.). Λ_M (acetone, 298 K, ohm^{-1} mol^{-1}cm^2): 142. IR (KBr, cm^{-1}): 3100–3040 (aromatic ν_{C-H}), 2980 2850 m/w (ν_{C-H}); 1600–1570 m (aromatic ν_{C-C} and ν_{C-N}); 1170–1000 s (ν_{BF4}). ^{1}H NMR ($CDCl_3$, 298 K) δ 9.17 (s, 1H, CH; ^{13}C HSQC 65.86), 8.40–8.00 (m, 4H, btz), 7.90–6.95 (m, 35H, Ph and PPh$_3$). ^{31}P {^{1}H} NMR ($CDCl_3$, 208 K) δ 0.08 (FWHM = 115 Hz).

Characterization of (**2**). Elemental analysis for $C_{55}H_{42}BCuF_4N_6OP_2$, calcd: C, 65.1%, H, 4.2%, N, 8.3%. Found: C, 64.8%, H, 4.2%, N, 8.3%. M.p. (°C): 160 (dec. > 230 °C). Λ_M (acetone, 298 K, ohm^{-1} mol^{-1}cm^2): 169. IR (KBr, cm^{-1}): 3100–3060 (aromatic ν_{C-H}), 2970–2850 m/w (ν_{C-H}), 1610–1570 m/s (aromatic ν_{C-C} and ν_{C-N}), 1160–1000 m (ν_{BF4}). ^{1}H NMR ($CDCl_3$, 298 K) δ 9.06 (s, 1H, CH), 7.80–6.50 (m, br, 41H, btz and Ph and DPEphos). ^{31}P {^{1}H} NMR ($CDCl_3$, 298 K) δ 15.45 (FWHM = 94 Hz).

Characterization of (**3**). Elemental analysis for $C_{37}H_{28}BCuF_4N_9P$, calcd: C, 51.7%, H, 3.3%, N, 14.5%. Found: C, 51.3%, H, 3.2%, N, 14.5%. M.p. (°C): 175 (dec. > 180 °C). Λ_M (acetone, 298 K, ohm^{-1} mol^{-1}cm^2): 126. IR (KBr, cm^{-1}): 3100–3005 m/w (aromatic ν_{C-H}), 2970–2850 m/w (ν_{C-H}), 1630–1560 m (aromatic ν_{C-C} and ν_{C-N}), 1170–1000 s (ν_{BF4}). ^{1}H NMR ($CDCl_3$, 298 K) δ 10.64 (s, 1H, br, CH), 7.75 (d, 3H, br, btz), 7.45–7.15 (m, 15H, br, phosphine), 6.67 (t, 3H, br, btz), 6.42 (t, 3H, br, btz), 6.06 (d, br). ^{31}P {^{1}H} NMR ($CDCl_3$, 218 K) δ −1.11 (FWHM = 125 Hz).

Characterization of (**4**). Elemental analysis for $C_{28}H_{34}BCuF_4N_9P$, calcd: C, 49.6%, H, 5.1%, N, 18.6%. Found: C, 49.4%, H, 5.1%, N, 18.5%. M.p. (°C): 140 (dec.). Λ_M (acetone, 298 K, ohm^{-1} mol^{-1}cm^2): 162. IR (KBr, cm^{-1}): 3100–3010 m/w (aromatic ν_{C-H}), 2970–2850 m/w (ν_{C-H}); 1640–1590 m (aromatic ν_{C-C} and ν_{C-N}); 1250–1150 s (ν_{BF4}). ^{1}H NMR ($CDCl_3$, 313 K) δ 10.59 (s, 1H, CH), 8.64 (s, 3H, br, btz), 8.10 (d, 3H, J_{HH} = 8 Hz, btz), 7.84 (t, 3H, J_{HH} = 8 Hz, btz), 7.54 (t, 3H, J_{HH} = 8 Hz, btz), 2.38 (m, 3H,

CH-phosphine), 1.44 (m, 18H, CH_3-phosphine). ^{31}P {^1H} NMR ($CDCl_3$, 298 K) δ 37.57 (FWHM = 360 Hz, br).

X-ray structure determination

Crystallographic data were collected at CACTI (Universidade de Vigo) at low temperature using a Bruker D8 Venture with a CMOS Photon 100 detector and Mo-Kα radiation (λ = 0.71073 Å) equipped with a CryoStream 800 system. The software APEX3 was used for collecting frames of data, indexing reflections and the determination of lattice parameters, SAINT for integration of intensity of reflections and SADABS for scaling and empirical absorption correction [45]. Further crystallographic treatment was performed with the Oscail program [46]. The structure of the compound was solved by using the SHELXT program [47] and refined by full-matrix least-squares based on F^2, SHELXL program [48]. Non-hydrogen atoms were refined with anisotropic displacement parameters. Hydrogen atoms were included in idealized positions and refined with isotropic displacement parameters. Further details concerning crystal data and structural refinement are given in Table 1. CCDC 1985082 contains the supplementary crystallographic data for this paper. These data can be obtained free of charge from the Cambridge Crystallographic Data Centre via www.ccdc.cam.ac.uk/data_request/cif. PLATON (version 220719) was used to obtain some geometrical parameters of the cif file [49], in particular hydrogen bonds and other weak intermolecular interactions [50–54].

Table 1 Crystallographic data

Compound	$CH(btz)_3$
Empirical formula	$C_{19}H_{13}N_9$
Formula weight	367.38
Temperature	100(2) K
Wavelength	0.71073 Å
Crystal system	Monoclinic
Space group	$P2_1/c$
Unit cell dimensions	a = 9.8330(8) Å
	b = 14.6452(10) Å
	c = 11.9477(9) Å
	β = 96.571(3)°
Volume	1709.2(2) Å^3
Z	4
Density (calculated)	1.428 Mg/m^3
Absorption coefficient	0.094 mm^{-1}
F(000)	760
Crystal size	0.235 × 0.035 × 0.029 mm
Θ range for data collection	2.209 to 28.345°
Index ranges	$-12 \le h \le 13$
	$-19 \le k \le 19$
	$-15 \le l \le 15$
Reflections collected	32,654
Independent reflections	4261 [R_{int} = 0.0560]
Reflections observed (> 2σ)	3295
Data Completeness	0.999
Absorption correction	Semi-empirical from equivalents
Max. and min. transmission	0.7457 and 0.6533
Refinement method	Full-matrix least-squares on F^2
Data/restraints/parameters	4261/0/253
Goodness of fit on F^2	1.055
Final R indices [$I > 2\sigma(I)$]	R_1 = 0.0426
	wR_2 = 0.0938
R indices (all data)	R_1 = 0.0635
	wR_2 = 0.1022
Largest diff. peak and hole	0.246 and −0.307 e.Å^{-3}

DFT calculations

The ground-state geometry optimization of [Cu{CHPh(btz)$_2$}(PPh$_3$)$_2$]$^+$ (**1**$^+$) and [Cu{CH(btz)$_3$}(PPh$_3$)]$^+$ (**3**$^+$) was carried out using the range-separated hybrid DFT functional ωB97X [55–57] in combination with Alhrichs' split-valence basis set def2-SVP [58]. The relative energies of the excited states were obtained by carrying out TD-DFT (time-dependent DFT) calculations at the same theoretical level using the ground-state geometry. The TD-DFT approach was also used for the geometry optimization of the first singlet and triplet excited states [59]. The software used was Gaussian 16 [60]. Cartesian coordinates of the DFT-optimized structures are given in Supplementary Data file.

Results and discussion

Polydentate benzotriazole-based ligands were synthesized accordingly to literature procedures (see Experimental section). To the best of our knowledge, the X-ray structure of tris(benzotriazol-1-yl)methane was never reported [61]. The compound consists of a helical built around the tertiary carbon atom substituted by three *N*-benzotriazolyl moieties. Figure 1 shows the ellipsoid plot of the compound [62], along with the numbering scheme used on one of the btz moieties. Although the structure resembles ligands such as classical tris(azolyl)borates [63], it is more related to known tris(azolyl)methane derivatives such as tris(pyrazolyl) methane [64] and its trimethyl [65] or dimethyl derivatives [66, 67]. Distances and angles in the compound are in the expected range and they can be retrieved from the CCDC, under the number 1985082. Selected data are given in Table 2. C(1)–N bonds are between 1.439(2) and 1.465(2) Å. The N–C–N angles are comprised between 109.4(1) and 113.3(1)°, typical of a sp^3 carbon atom. C(1) is 0.448(2) Å over the N(11)–N(21)–N(31) plane. The benzotriazole rings

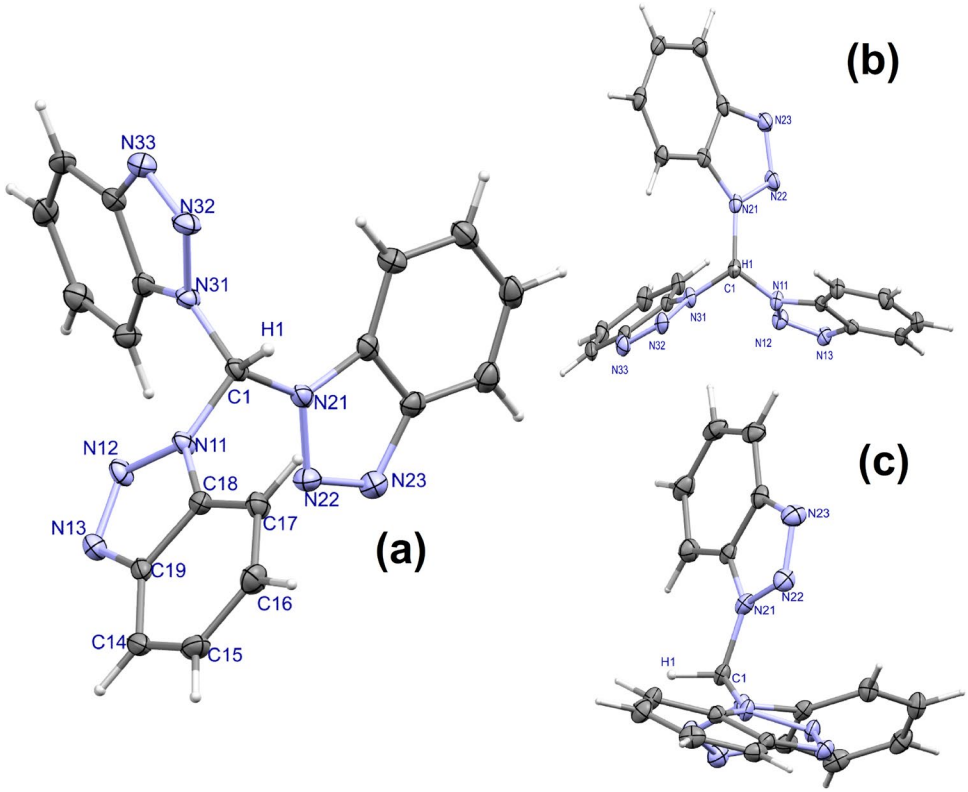

Fig. 1 Ellipsoid plot (50% probability level) of $CH(btz)_3$ (**a**) and views along the C(1)–H(1) bond (**b**) and 90° y-rotated (**c**)

Table 2 Bond lengths [Å] and angles [°] around C(1) for $CH(btz)_3$

C(1)–N(31)	1.4392(16)	N(31)–C(1)–N(11)	113.28(10)
C(1)–N(21)	1.4650(17)	N(11)–C(1)–N(21)	109.40(10)
C(1)–N(11)	1.4394(16)	N(31)–C(1)–N(21)	109.96(10)

are more or less planar. The root mean square deviation from the planarity for the 8 atoms implicated is between 0.0064 and 0.0149 Å. The propeller-shaped arrangement is not regular and the pseudo-C_3 symmetry is broken, in part because one of the benzotriazole rings is upwards, in the same direction of the C(1)–H(1) bond. This situation is described as *ABB* conformation for tris(triazolyl)methane [66, 67]. The *ABB* conformation is, however, not the only distortion in the helical arrangement. As observable in the insets of Fig. 1, two benzotriazole rings are in opposite directions. Moreover, the dihedral angles between the N(11)–N(21)–N(31) plane and the three benzotriazol-1-yl planes are different. The benzotriazole rings containing N(11) (btz#1) and N(31) (btz#3) form dihedral angles of 73.22(4)° and 82.11(3)°, respectively. The ring containing N(21) (btz#2) breaks the helicoid arrangement because it is much more perpendicular to the N(11)–N(21)–N(31) plane, forming a dihedral angle of 33.40(5)°. The dihedral angle between the perfect plane H(1)–C(1)–N(31) and the corresponding btz#3 ring is only 7.85(3)°, and between H(1)–C(1)–N(11) and btz#1, it is 24.19(8)°. The dihedral angle increases up to 59.65(5)° on considering the H(1)–C(1)–N(21) plane and btz#2. Dihedral angles of 23, 29 and 62° were used by Ochando et al. to define the *ABB* conformation of tris(3,5-dimethylpyrazol-1-yl)methane [66, 67].

The supramolecular structure is basically maintained by some π,π-stacking between the rings [68]. The most important ones imply the btz#3 triazole ring and its symmetry related [$1-x$, $1-y$, $1-z$], and the btz#1 benzene ring and its symmetry related [$1-x$, $-y$, $1-z$]. The two interactions cause a growth along the *b* axis (see Fig. S1). The distances between the centroids are 3.4298(8) and 3.7669(8) Å, and the ring slippage values are 1.281 and 1.592 Å, respectively. Probably because of its different orientation btz#2 is unable to form π,π-stacking interactions, and only C–H···π interactions at each side of the benzene ring are found (H–centroid–H angle of 165.6°) [69], as shown in Fig. S2. The C–H···π interaction with the close H(35) [symm. op. $2-x$, $1-y$, $1-z$] generates dimeric entities, while that with H(37) atom [symm. op. x, $1/2-y$, $1/2+z$] generates a growing in the *c* axis (see Fig. S2). The parameters are given in Table S1.

Heteroleptic Cu(I) complexes with bis(benzotriazol-1-yl) phenylmethane in the coordination sphere, (**1**) and (**2**), were obtained from the reaction of the proper Cu(I) borohydride complex with the ligand and $HBF_4{\cdot}Et_2O$ under mild conditions. Complexes with tris(benzotriazol-1-yl)methane and

phosphines, (**3**) and (**4**), were instead obtained by the subsequent addition of the ligands to the precursor $[Cu(NCCH_3)_4][BF_4]$ (see Scheme 1).

Elemental analyses are in agreement with the proposed formulae, and conductivity measurements in acetone solutions indicate that the complexes behave as 1:1 electrolytes. The evolution of the reactions was confirmed by the IR spectra, where no signal attributable to coordinated borohydride or acetonitrile is detectable. The IR bands are related to vibrations of the coordinated N- and P-donor ligands, superimposed to ν_{BF4} in the 1000–1170 cm^{-1} range. The presence of the counter-anion is further confirmed by the appearance of a quintet ($^1J_{BF}$ = 0.9 Hz) in the ^{11}B NMR spectra. Diagnostic for the presence of bis(benzotriazol-1-yl)phenylmethane or tris(benzotriazol-1-yl)methane in the coordination sphere is the methine ^1H NMR resonance, observable in the high-frequency regions of the spectra between 9.06 and 10.64 ppm. The remaining ^1H NMR signals fall in the aromatic region and are related to the phosphine substituents and to the benzotriazol-1-yl or phenyl substituents of the N-donor ligands. The only exception is the ^1H NMR spectrum of (**4**), with multiplets affected by the temperature in the aliphatic region related to the isopropyl substituents of the phosphine. The coordination of mono- and bidentate phosphines is confirmed by the $^{31}P\{^1H\}$ NMR spectra, showing in all the cases only a broad resonance also at low temperature, this indicating fluxional behaviour in solution.

The complexes are characterized by absorptions for wavelengths below 400 nm in diluted CH_2Cl_2 solutions, with molar extinction coefficients higher than 30,000 M^{-1} cm^{-1} in the presence of aromatic phosphines. The tails in the visible range account for the yellow colour observed for concentrated solutions and powder samples. On the basis of the comparison with the free ligands, the absorption spectra are almost in part related to the $\pi^* \leftarrow \pi$ transitions of the aromatic fragments, but DFT calculations (see below) suggest the superimposition of MLCT transitions that are, however, not distinguishable in the UV–VIS spectra (see Fig. S3).

Excitation of powder samples can be achieved with near-UV and violet light (see the PLE spectra in Fig. 2), affording bright yellow and orange emissions centred between 555 and 600 nm, as observable in the PL spectra reported in Fig. 2. The emission maxima fall at longer wavelengths for the tris(benzotriazol-1-yl)methane derivatives. The PL and PLE bands of (**1**) and (**2**) are roughly comparable to those recently reported for the homoleptic bis(indazol-1-yl)phenylmethane complex $[Cu(N^N)_2]^+$ [39]. The wider range of the solid-state PLE spectra with respect to the solution absorption spectra can be interpreted on the basis of the enhancement of the MLCT transitions described below. The luminescence is not maintained in solution. Absorption and emission data of the complexes are given in Table 3. Photoluminescent quantum yield (ϕ) values depend upon the

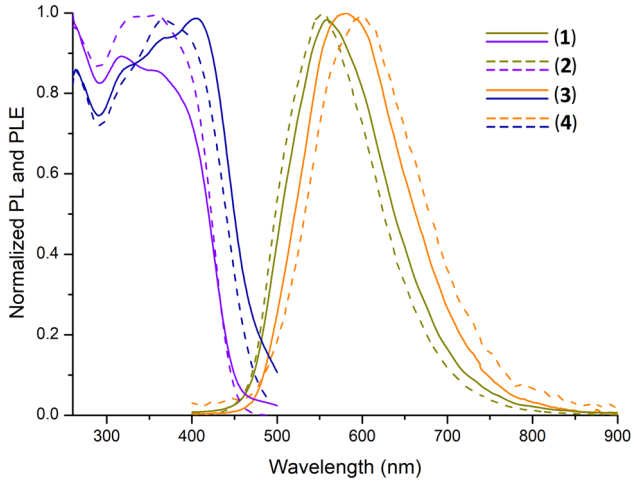

Fig. 2 Normalized PL (solid sample, $\lambda_{excitation}$ = 375 nm, r.t.): solid dark yellow line, (**1**); dashed dark yellow line, (**2**); solid orange line, (**3**); dashed orange line, (**4**). Normalized PLE (solid sample, $\lambda_{emission}$ = 600 nm, r.t.): solid violet line, (**1**); dashed violet line, (**2**); solid dark blue line, (**3**); dashed dark blue line, (**4**)

choice of the ancillary ligands and the rigidity of the resulting complexes. The highest values were measured for (**2**) (22%) and (**3**) (13%) (Table 3). In particular, the intensity of emission appreciably grows by replacing the two triphenylphosphine ligands with DPEphos in the coordination sphere. Such a trend was previously observed for similar compounds [70–72] and it is probably attributable to the rigidity and to the steric hindrance of the chelating phosphine that contributes to prevent distortions at the excited state, thus improving the luminescent properties. As a further comparison, the emission of (**4**) is lower than that of (**3**), perhaps because of the more flexible isopropyl substituents. The heteroleptic complexes here described are, with the exception of (**4**), appreciably more luminescent than the homoleptic bis(indazol-1-yl)phenylmethane complex $[Cu(N^N)_2]^+$ (ϕ = 1.3%) [39] .

DFT calculations on ground-state singlet ($\mathbf{1}^+$) and ($\mathbf{3}^+$) indicate that the lowest energy singlet–singlet light absorption is related to the charge transfer from frontier occupied metal- and phosphine-centred orbitals and unoccupied π^* orbitals of the benzotriazole fragments, therefore ^{1}MLCT nature can be attributed (see Fig. 3). Selected computed bond lengths are given in Table 4.

The large Stokes shifts, about 200 nm, and the wide emission bands (FWHM between 4100 and 4200 cm^{-1}) suggest that the emissions of the complexes could involve excited states with triplet multiplicity. The luminescence decay curves show bi-exponential behaviour, with a fast component (τ < 500 ns) and a slow component in the tenth of microseconds range. Selected curves are provided in Fig. S4. The slow component is appreciably longer for the complexes

Table 3 Absorption and emission data of the complexes

	[a] UV–VIS, nm (ε: M^{-1} cm^{-1})	[b] PL, nm (FWHM: cm^{-1})	[c] PLE, nm	[d] ϕ%	[e] τ (μs)
(**1**)	< 310, 255 (ε = 34,100), 262 (sh), 274 (sh)	565 (FWHM = 4100)	< 460	7	< 0.5, ≈ 30
(**2**)	< 400, 260 (ε = 33,400), 270 (sh)	555 (FWHM = 4100)	< 460	22	< 0.5, ≈ 40
(**3**)	< 375, 262 (ε = 33,200), 269 (sh)	582 (FWHM = 4200)	< 500	13	< 0.5, ≈ 140
(**4**)	< 375, 262 (ε = 22,800), 257 (sh), 279 (sh)	599 (FWHM = 4100)	< 500	2	< 0.5, ≈ 120

[a] CH_2Cl_2 solution, 298 K.[b] Powder samples, r.t., $\lambda_{excitation}$ = 375 nm.[c] Powder samples, r.t., $\lambda_{emission}$ = 586 nm (**1**), 560 (**2**), 600 (**3**), 630 (**4**).[d] Powder samples, r.t. [e] Powder samples, r.t., $\lambda_{excitation}$ = 290 nm

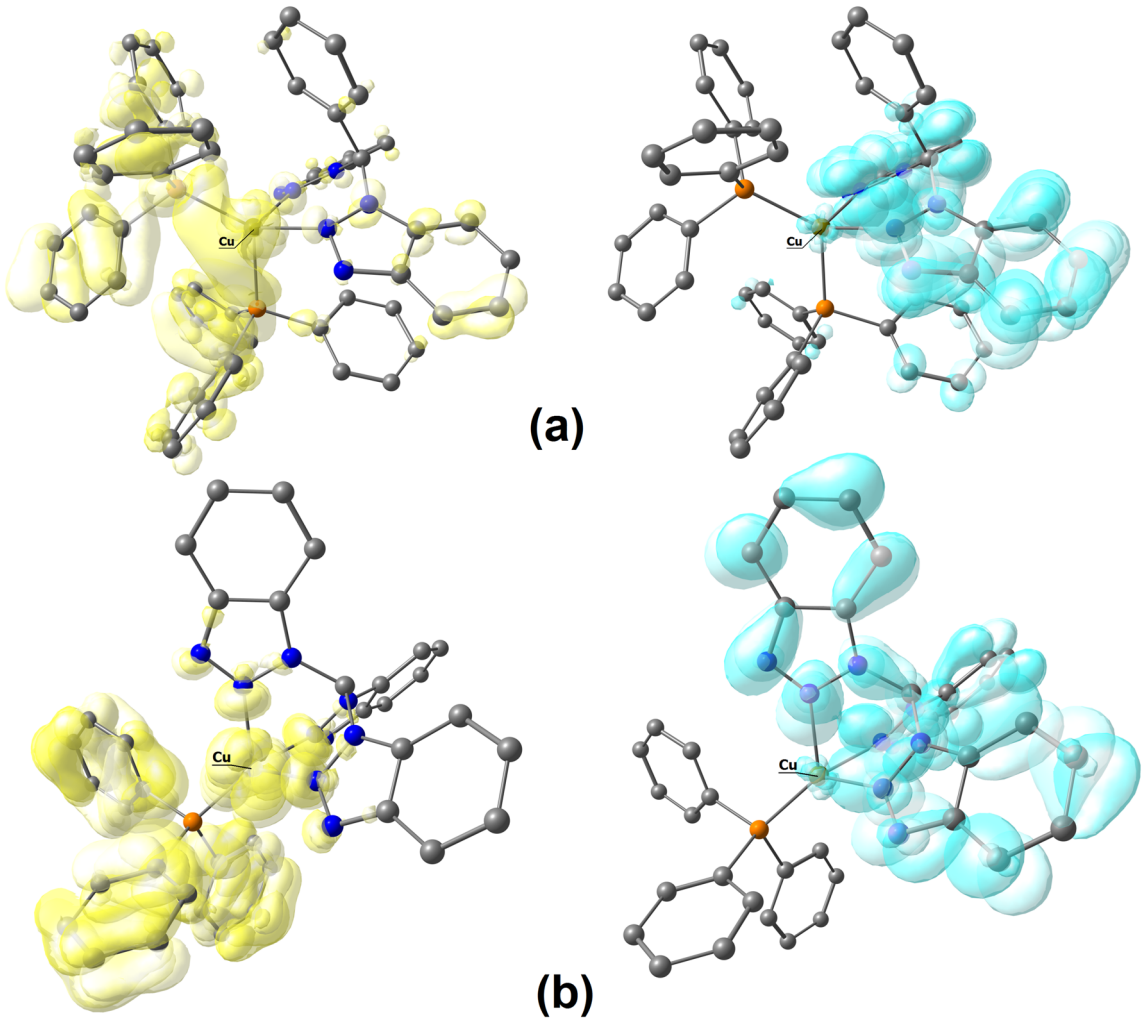

Fig. 3 DFT-optimized structures of singlet ($\mathbf{1}^+$) (**a**) and ($\mathbf{3}^+$) (**b**) and superposition of occupied (yellow tones) and unoccupied (cyan tones) orbitals involved in the lowest energy singlet–singlet absorptions. **a** Occupied: HOMO, HOMO–1, HOMO−8; unoccupied: LUMO, LUMO + 1, LUMO + 18. **b** Occupied: HOMO-3, HOMO-4, HOMO-6, HOMO-7; unoccupied: LUMO, LUMO + 1. Surface isovalue = 0.03 a.u

with tris(benzotriazol-1-yl)methane in the coordination sphere (see Table 3).

In order to investigate the transitions from a computational point of view, the triplet state geometries of the complexes were optimized. Selected data are given in Table 4. The lowest energy singlet–triplet absorptions implicate the molecular orbitals superimposed in Fig. 4. The triplet state emissions are the specular processes and appear based on transitions between benzotriazole-centred orbitals and molecular orbitals localized on the metal centre, the

Table 4 Selected computed bond lengths and angles

Compound	Lengths (Å)	Angles (°)
($\mathbf{1}^+$) Singlet	Cu–N 2.156, 2.210 Cu–P 2.283, 2.333	N–Cu–N 87.1 P–Cu–P 122.5
($\mathbf{1}^+$) Triplet	Cu–N 1.921, 2.125 Cu–P 2.337, 2.341	N–Cu–N 91.8 P–Cu–P 105.0
($\mathbf{3}^+$) Singlet	Cu–N 2.176, 2.176, 2.178 Cu–P 2.218	P–Cu–N 129.0, 129.3, 129.4 N–Cu–N 84.1, 84.3, 84.3
($\mathbf{3}^+$) Triplet	Cu–N 2.100, 2.202, 2.203 Cu–P 2.218	P–Cu–N 127.8, 127.9, 131.8 N–Cu–N 82.8, 84.9, 85.1

phosphine ligands and also the N-donor ligands (see Fig. 4). The computed values, respectively, 563 and 678 nm for ($\mathbf{1}^+$) and ($\mathbf{3}^+$), are roughly in agreement with the experimental data. The nature of the emissions assigned on the basis of DFT calculations is therefore ^{3}MLCT/^{3}LC. The presence of a fast component in the luminescence decay curves allows, however, to suppose that also excited states with singlet multiplicity could be involved in the observed emissions.

Yellow-emitting compounds with wide emission bands are of interest for the preparation of white light emitting diodes (WLEDs). A common technological approach is the coating of blue LEDs with yellow-emitting species, used for

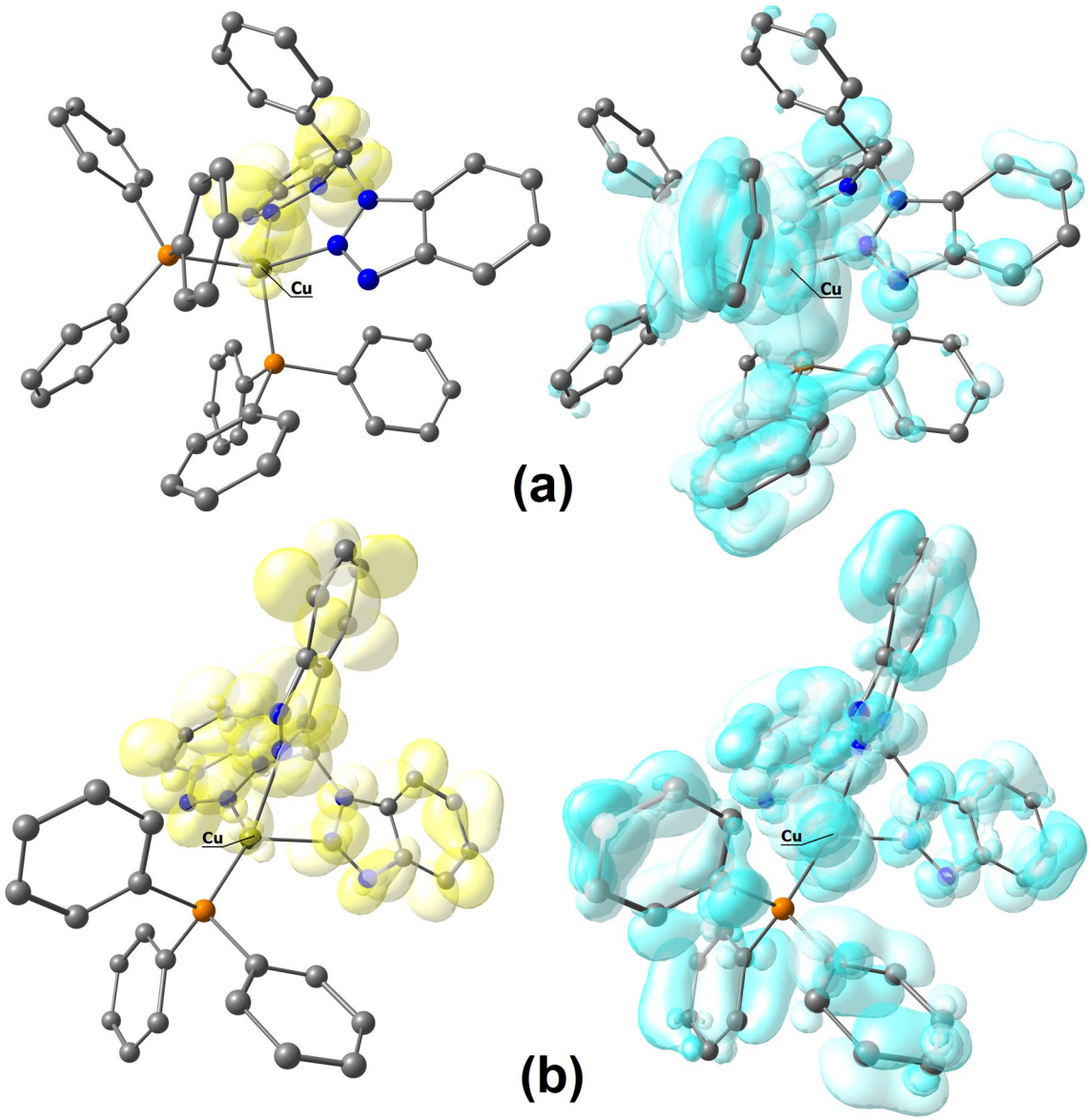

Fig. 4 DFT-optimized structures of triplet ($\mathbf{1}^+$) (**a**) and ($\mathbf{3}^+$) (**b**) and superposition of occupied (cyan tones) and unoccupied (yellow tones) orbitals involved in the lowest energy singlet–triplet absorptions. **a** Occupied: HOMO, HOMO-1, HOMO-10, HOMO-14, HOMO-22; unoccupied: LUMO. **b** Occupied: HOMO-5, HOMO-6, HOMO-8, HOMO-10, HOMO-12, HOMO-16; unoccupied: LUMO, LUMO + 2. Surface isovalue = 0.03 a.u

instance in the case of indium gallium nitride (InGaN) LEDs in combination with cerium-doped yttrium aluminium garnet (YAG:Ce^{3+}) [73]. The PL and PLE spectra of the yellow-emitting bis(benzotriazol-1-yl)phenylmethane derivatives suggested their possible application in this field, supported by the thermal stability of the DPEphos complex (**2**). As shown in Fig. 5, the decomposition starts at temperatures above 250 °C. The other compounds are characterized by lower thermal stability, as observable from the TGA curves given in Fig. S5.

Compound (**2**) maintains its luminescence without meaningful alterations once embedded in poly(methyl methacrylate) (PMMA) matrix (see Fig. 5 for a comparison between powder and doped PMMA). The doped polymers obtained from dichloromethane solutions were applied for the coating of commercial UV LEDs with emission maximum at 385 nm. The emission spectrum of a typical coated LED is reported in Fig. 6. White light is conventionally located at coordinates $x = y = 0.333$, while (**2**) and the derived WLED are, respectively, positioned at $x = 0.444$, $y = 0.512$ and $x = 0.354$, $y = 0.381$ in the CIE 1931 diagram (see Fig. 6). The white emission thus obtained is characterized by a colour temperature of 4800 K, calculated accordingly to McCamy's formula [74].

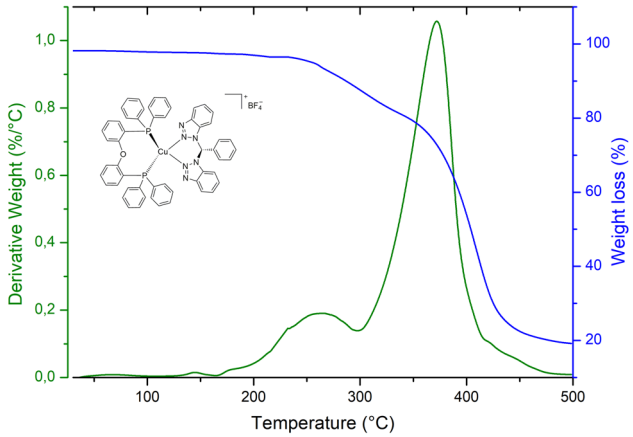

Fig. 5 TGA curve of (**2**) (blue line: weight loss percentage; green line: first derivative of TGA curve)

Conclusions

The results summarized in this work evidence that ligands containing the benzotriazole heterocycle are suitable for the preparation of new Cu(I) complexes. Heteroleptic coordination compounds containing bi- or tridentate N-donors and phosphines in the coordination sphere are appreciably luminescent in the yellow–orange range. As highlighted by DFT calculations, the empty molecular orbitals on the benzotriazol-1-yl fragments play a role of paramount importance in the absorption and emission features of the corresponding complexes. The emission maximum mainly depends upon the nature of the atoms composing the first coordination sphere of Cu(I). In summary, both the coordinating ability and the electronic features of benzotriazole make this azole well suited for the

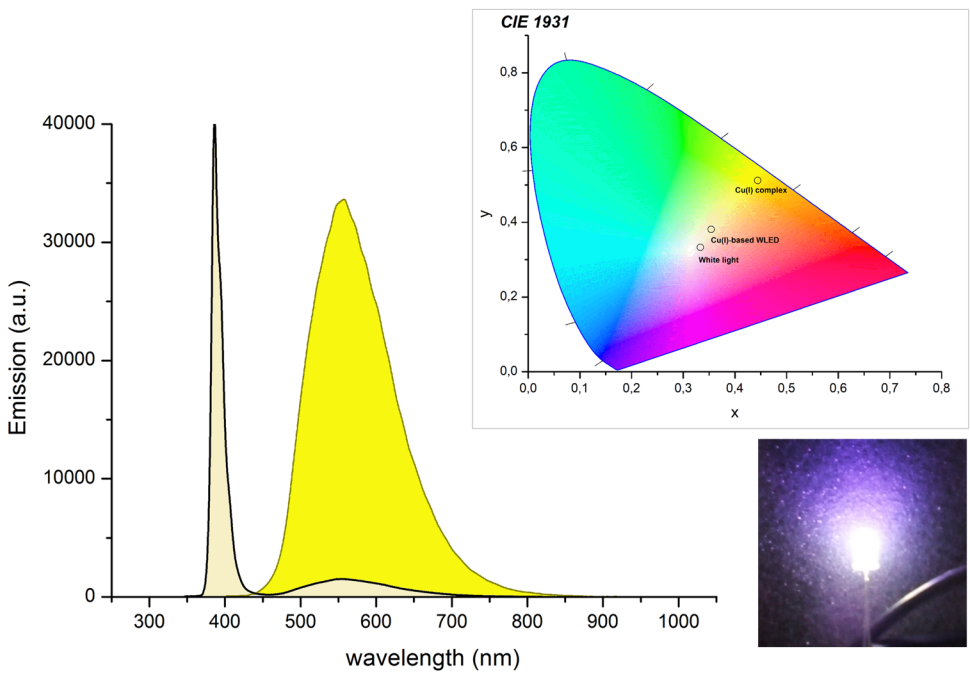

Fig. 6 Emission spectra of (**2**) (yellow filled) and of Cu(I)-based WLED (whitish filled). Inset: CIE 1931 chromaticity diagram with the chromaticity coordinates of white light, (**2**) and the related WLED

development of Cu(I) complexes of possible interest in the fields of optics and lighting.

Supplementary data

Intermolecular interactions of tris(benzotriazol-1-yl-methane in the crystal structure (Figs. S1–S2, Table S1). Absorption spectra of diluted CH_2Cl_2 solutions of the complexes, Fig. S3. Selected luminescence decay curves, Figure S4. TGA curves of the complexes (Fig. S5). Cartesian coordi-nates of the DFT-optimized structures (Tables S2–S3).

Acknowledgements CACTI (University of Vigo) is gratefully acknowledged for X-ray data collection. We acknowledge Università Ca' Foscari Venezia for financial support (Bando Spin 2018, D. R. 1065/2018 prot. 67416) and CINECA (COLUMN project 2020) for the availability of computing resources.

References

1. Wenger OS (2018) Photoactive complexes with earth-abundant metals. J Am Chem Soc 140:13522–13533. https://doi.org/10.1021/jacs.8b08822
2. Zhang QC, Xiao H, Zhang X, Xu LJ, Chen ZN (2019) Luminescent oligonuclear metal complexes and the use in organic light-emitting diodes. Coord Chem Rev 378:121–133. https://doi.org/10.1016/j.ccr.2018.01.017
3. Costa RD, Ortí E, Bolink HJ, Monti F, Accorsi G, Armaroli N (2012) Luminescent ionic transition-metal complexes for light-emitting electrochemical cells. Angew Chem Int Ed 51:8178–8211. https://doi.org/10.1002/anie.201201471
4. Bizzarri C, Spuling E, Knoll DM, Volz D, Bräse S (2018) Sustainable metal complexes for organic light-emitting diodes (OLEDs). Coord Chem Rev 373:49–82. https://doi.org/10.1016/j.ccr.2017.09.011
5. Cariati E, Lucenti E, Botta C, Giovanella U, Marinotto D, Righetto S (2016) Cu(I) hybrid inorganic–organic materials with intriguing stimuli responsive and optoelectronic properties. Coord Chem Rev 306:566–614. https://doi.org/10.1016/j.ccr.2015.03.004
6. Armaroli N, Accorsi G, Cardinali F, Listorti A (2007) Photochemistry and photophysics of coordination compounds: copper. Top Curr Chem 280:69–115. https://doi.org/10.1007/128_2007_128
7. Tao Y, Yuan K, Chen T, Xu P, Li H, Chen R, Zheng C, Zhang L, Huang W (2014) Thermally activated delayed fluorescence materials towards the breakthrough of organoelectronics. Adv Mater 26:7931–7958. https://doi.org/10.1002/adma.201402532
8. Yersin H, Rausch AF, Czerwieniec R, Hofbeck T, Fischer T (2011) The triplet state of organo-transition metal compounds. Triplet harvesting and singlet harvesting for efficient OLEDs. Coord Chem Rev 255:2622–2652. https://doi.org/10.1016/j.ccr.2011.01.042
9. Yersin H (2018) Highly efficient OLEDs: materials based on thermally activated delayed fluorescence. Wiley-VCH, Weinheim
10. McMillin DR, Buckner MT, Ahn BT (1977) A light-induced redox reaction of bis(2,9-dimethyl-1,10-phenanthroline)copper(I). Inorg Chem 16:943–945. https://doi.org/10.1021/ic50170a046
11. Buckner MT, McMillin DR (1978) Photoluminescence from copper(I) complexes with low-lying metal-to-ligand charge transfer excited states. J Chem Soc Chem Commun, pp 759–761. https://doi.org/10.1039/C39780000759
12. Blaskie MW, McMillin DR (1980) Photostudies of copper(I) systems. 6. Room-temperature emission and quenching studies of bis(2,9-dimethyl-1,10-phenanthroline)copper(I). Inorg Chem 19:3519–3522. https://doi.org/10.1021/ic50213a062
13. Scaltrito DV, Thompson DW, O'Callaghan JA, Meyer GJ (2000) MLCT excited states of cuprous bis-phenanthroline coordination compounds. Coord Chem Rev 208:243–266. https://doi.org/10.1016/S0010-8545(00)00309-X
14. Lavie-Cambot A, Cantuela M, Leydet Y, Jonusauskas G, Bassani DM, McClenaghan ND (2008) Improving the photophysical properties of copper(I) bis(phenanthroline) complexes. Coord Chem Rev 252:2572–2584. https://doi.org/10.1016/j.ccr.2008.03.013
15. Liu Y, You SC, Ho CL, Wong WY (2018) Recent advances in copper complexes for electrical/light energy conversion. Coord Chem Rev 375:514–557. https://doi.org/10.1016/j.ccr.2018.05.010
16. Si Z, Li J, Li B, Liu S, Li W (2009) High light electroluminescence of novel Cu(I) complexes. J Lumin 129:181–186. https://doi.org/10.1016/j.jlumin.2008.09.014
17. Min J, Zhang Q, Sun W, Cheng Y, Wang L (2011) Neutral copper(I) phosphorescent complexes from their ionic counterparts with 2-(2′-quinolyl)benzimidazole and phosphine mixed ligands. Dalton Trans 40:686–693. https://doi.org/10.1039/C0DT01031F
18. Bergmann L, Braun C, Nieger M, Bräse S (2018) The coordination- and photochemistry of copper(I) complexes: variation of N^N ligands from imidazole to tetrazole. Dalton Trans 47:608–621. https://doi.org/10.1039/C7DT03682E
19. Gérardy R, Monbaliu JCM (2016) Preparation, reactivity, and synthetic utility of simple benzotriazole derivatives. The chemistry of benzotriazole derivatives. Topics in Heterocyclic Chemistry 43:1–66. https://doi.org/10.1007/7081_2015_179
20. Katritzky AR, Rogovoy BV (2003) Benzotriazole: an ideal synthetic auxiliary. Chem Eur J 9:4586–4593. https://doi.org/10.1002/chem.200304990
21. Loukopoulos E, Kostakis GE (2019) Recent advances in the coordination chemistry of benzotriazole-based ligands. Coord Chem Rev 395:193–229. https://doi.org/10.1016/j.ccr.2019.06.003
22. Richardson C, Steel PJ (2003) Benzotriazole as a structural component in chelating and bridging heterocyclic ligands; ruthenium, palladium, copper and silver complexes. Dalton Trans, pp 992–1000. https://doi.org/10.1039/b206990c
23. Peresypkina EV, Lider EV, Smolentsev AI, Sanchiz J, Gil-Hernández B, Potapov AS, Khlebnikov AI, Kryuchkova NA, Lavrenova LG (2012) Bis(benzotriazol-1-yl)methane as a linker in the assembly of new copper(II) coordination polymers: Synthesis, structure and investigations. Polyhedron 48:253–263. https://doi.org/10.1016/j.poly.2012.08.072
24. Belousov YA, Goncharenko VE, Bondarenko GN, Ganina OG, Bezzubov SI, Taidakov IV (2020) Linear metal-organic frameworks based on Bis(1-Benzotriazolyl)methane and zinc and copper nitrates. Russ J Coord Chem 46:805–811. https://doi.org/10.1134/S1070328420080023
25. Lobbia GG, Pellei M, Pettinari C, Santini C, Somers N, White AH (2002) Poly(1,2,3-benzotriazolyl)borate complexes with copper(I) and tri-organophosphane: an unprecedented κ^1-coordination of $[H_2B(btz)_2]$ (btz=1,2,3-benzotriazolyl) in the X-ray crystal structure of $[Cu(PBn_3)_2\{(btz)BH_2(btz)\}]$. Inorg Chim Acta 333:100–108. https://doi.org/10.1016/S0020-1693(02)00774-0

26. Avila L, Elguero J, Juliá S, del Mazo JM (1983) N-Polyazolymethanes. IV. Reaction of Benzotriazole with Methylene Chloride and Chloroform under Phase Transfer Conditions. Heterocycles 20:1787–1792. https://doi.org/10.3987/R-1983-09-1787
27. Elguero J, Claramunt RM, Garcerán R, Julià S, Aliva L, del Mazo JM (1987) 13C NMR study of polyphenyl-, poly-*N*-azolyl-and poly-*N*-benzazoyl-methanes. Magn Reson Chem 25:260–268. https://doi.org/10.1002/mrc.1260250317
28. Katritzky AR, Xie L (1996) *para*-Formylation of nitroarenes via vicarious nucleophilic substitution of hydrogen with tris(benzotriazol-1-yl)methane. Tetrahedron Lett 37:347–350. https://doi.org/10.1016/0040-4039(95)02169-8
29. Katritsky AR, Wu H, Xie L (1997) Novel tele nucleophilic aromatic substitutions in α-(benzotriazol-1-yl)alkyl aryl ketones. Tetrahedron Lett 38:903–906. https://doi.org/10.1016/S0040-4039(96)02455-0
30. Androsov DA, Neckers DC (2007) Photochemical study of Tris(benzotriazol-1-yl)methane. J Org Chem 72:1148–1152. https://doi.org/10.1021/jo061851d
31. Bortoluzzi M, Castro J, Enrichi F, Vomiero A, Busato M, Huang W (2018) Green-emitting manganese (II) complexes with phosphoramide and phenylphosphonic diamide ligands. Inorg Chem Comm 92:145–150. https://doi.org/10.1016/j.inoche.2018.04.023
32. Bortoluzzi M, Castro J, Trave E, Dallan D, Favaretto S (2018) Orange-emitting manganese(II) complexes with chelating phosphine oxides. Inorg Chem Commun 90:105–107. https://doi.org/10.1016/j.inoche.2018.02.018
33. Bortoluzzi M, Castro J, Girotto M, Enrichi F, Vomiero A (2019) Luminescent copper(I) coordination polymer with 1-methyl-1H-benzotriazole, iodide and acetonitrile as ligands. Inorg Chem Comm 102:141–146. https://doi.org/10.1016/j.inoche.2019.02.016
34. Bortoluzzi M, Castro J (2019) Dibromomanganese(II) complexes with hexamethylphosphoramide and phenylphosphonic bis(diamide) ligands. J Coord Chem 72:309–327. https://doi.org/10.1080/00958972.2018.1560430
35. Bortoluzzi M, Castro J, Gobbo A, Ferraro V, Pietrobon L, Antoniutti (2020) Tetrahedral photoluminescent manganese(II) halide complexes with 1,3-dimethyl-2-phenyl-1,3-diazaphospholidine-2-oxide as a ligand. New J Chem 44:571–579. https://doi.org/10.1039/c9nj05083c
36. Bortoluzzi M, Castro J, Gobbo A, Ferraro V, Pietrobon L (2020) Light harvesting indolyl-substituted phosphoramide ligand for the enhancement of Mn(II) luminescence. Dalton Trans 49:7525–7534. https://doi.org/10.1039/d0dt01659d
37. Bortoluzzi M, Ferraro V, Castro J (2021) Synthesis and photoluminescence of manganese(II) naphtylphosphonic diamide complexes. Dalton Trans 50:3132–3136. https://doi.org/10.1039/D1DT00123J
38. Ferraro V, Bortoluzzi M, Castro J (2019) Synthesis of Bis(benzotriazol-1-yl)methane derivatives by Cobalt-catalyzed formation of C-C bonds. Proceedings 41:29. https://doi.org/10.3390/ecsoc-23-06469.
39. Ferraro V, Bortoluzzi M, Castro J, Vomiero A, You S (2020) Luminescent Cu(I) complex with bis(indazol-1-yl)phenylmethane as chelating ligand. Inorg Chem Commun 116:107894. https://doi.org/10.1016/j.inoche.2020.107894
40. Armarego WLF, Perrin DD (1996) Purification of laboratory chemicals, 4th edn. Butterworth-Heinemann, Oxford
41. Keller RN, Wycoff HD, Marchi LE (1946) Copper(I) chloride. Inorg Synth 2:1–4. https://doi.org/10.1002/9780470132333.ch1
42. Kubas GJ, Monzyk B, Crumblis AL (1990) Tetrakis(Acetonitrile) Copper(1+) Hexafluorophosphate(1-). Inorg Synth 28:68–70. https://doi.org/10.1002/9780470132593.ch15
43. Bianchini C, Ghilardi CA, Meli A, Midollini S, Orlandini A (1985) Reactivity of copper(I) tetrahydroborates toward carbon dioxide and carbonyl sulfide. Structure of (triphos)Cu(η^1-O_2CH). Inorg Chem 24:924–931. https://doi.org/10.1021/ic00200a025
44. Katritzky AR, Yang Z, Lam JN (1990) Tris(benzotriazol-1-yl) methane: A -CO_2H synthon for the preparation of carboxylic acids. Synthesis 8:666–669. https://doi.org/10.1055/s-1990-26975
45. Bruker (2015) APEX3, SMART, SAINT. Bruker AXS Inc., Madison, Wisconsin, USA
46. McArdle P (2017) Oscail, a program package for small-molecule single-crystal crystallography with crystal morphology prediction and molecular modelling. J Appl Cryst 50:320–326. https://doi.org/10.1107/S1600576716018446
47. Sheldrick GM (2015) SHELXT—Integrated space-group and crystal-structure determination. Acta Crystallogr A 71:3–8. https://doi.org/10.1107/S2053273314026370
48. Sheldrick GM (2015) Crystal structure refinement with SHELXL. Acta Crystallogr C 71:3–8. https://doi.org/10.1107/S2053229614024218
49. Spek AL (2009) Structure validation in chemical crystallography. Acta Crystallogr D 65:148–155. https://doi.org/10.1107/S090744490804362X
50. Grabowski SJ (2011) What is the covalency of hydrogen bonding? Chem Rev 111:2597–2625. https://doi.org/10.1021/cr800346f
51. Grabowski SJ (2016) Analysis of hydrogen bonds in crystals. Crystals 6:59 https://doi.org/10.3390/cryst6050059
52. Taylor R (2014) Which intermolecular interactions have a significant influence on crystal packing? CrystEngComm 16:6852–6865. https://doi.org/10.1039/C4CE00452C
53. Taylor R (2016) It isn't, it is: the C-H···X (X = O, N, F, Cl) interaction really is significant in crystal packing. Cryst Growth Des 16:4165–4168. https://doi.org/10.1021/acs.cgd.6b00736
54. Aakeröy CB, Champness NR, Janiak C (2010) Recent advances in crystal engineering. CrystEngComm 12:22–43. https://doi.org/10.1039/B919819A
55. Gerber IC, Ángyán JC (2005) Hybrid functional with separated range. Chem Phys Lett 415:100–105. https://doi.org/10.1016/j.cplett.2005.08.060
56. Chai JD, Head-Gordon M (2008) Long-range corrected hybrid density functionals with damped atom–atom dispersion corrections. Phys Chem Chem Phys 10:6615–6620. https://doi.org/10.1039/B810189B
57. Minenkov Y, Singstad Å, Occhipinti G, Jensen VR (2012) The accuracy of DFT-optimized geometries of functional transition metal compounds: a validation study of catalysts for olefin metathesis and other reactions in the homogeneous phase. Dalton Trans 41:5526–5541. https://doi.org/10.1039/C2DT12232D
58. Weigend F, Ahlrichs R (2005) Balanced basis sets of split valence, triple zeta valence and quadruple zeta valence quality for H to Rn: Design and assessment of accuracy. Phys Chem Chem Phys 7:3297–3305. https://doi.org/10.1039/B508541A
59. Ullrich CA (2012) Time-dependent density functional theory. Oxford University Press, Oxford
60. Frisch MJ, Trucks GW, Schlegel HB, Scuseria GE, Robb MA, Cheeseman JR, Scalmani G, Barone V, Petersson GA, Nakatsuji H, Li X, Caricato M, Marenich AV, Bloino J, Janesko BG, Gomperts R, Mennucci B, Hratchian HP, Ortiz JV, Izmaylov AF, Sonnenberg JL, Williams-Young D, Ding F, Lipparini F, Egidi F, Goings J, Peng B, Petrone A, Henderson T, Ranasinghe D, Zakrzewski VG, Gao J, Rega N, Zheng G, Liang W, Hada M, Ehara M, Toyota K, Fukuda R, Hasegawa J, Ishida M, Nakajima T, Honda Y, Kitao O, Nakai H, Vreven T, Throssell K, Montgomery JA Jr., Peralta JE, Ogliaro F, Bearpark MJ, Heyd JJ, Brothers EN, Kudin KN, Staroverov VN, Keith TA, Kobayashi R, Normand J, Raghavachari K, Rendell AP, Burant JC, Iyengar SS, Tomasi J, Cossi M, Millam J, Klene M, Adamo C, Cammi R, Ochterski JW, Martin RL, Morokuma K, Farkas O, Foresman JB, Fox DJ (2016) Gaussian 16, Revision C.01, Gaussian, Inc., Wallingford CT.

61. Groom CR, Bruno IJ, Lightfoot MP, Ward SC (2016) The Cambridge structural database. Acta Crystallogr B72:171–179. https://doi.org/10.1107/S2052520616003954
62. Macrae CF, Bruno IJ, Chisholm JA, Edgington PR, McCabe P, Pidcock E, Rodriguez-Monge L, Taylor R, van de Streek J, Wood PA (2008) Mercury CSD 2.0—new features for the visualization and investigation of crystal structures. J Appl Cryst 41:466–470. https://doi.org/10.1107/S0021889807067908
63. Lu D, Tang H (2015) Theoretical survey of the ligand tunability of poly(azolyl)borates. Phys Chem Chem Phys 17:17027–17033. https://doi.org/10.1039/C5CP02094H
64. Kerscher T, Pust P, Betz R, Klüfers P, Mayer P (2009) Trispyrazol-1-ylmethane. Acta Crystallogr E 65:o108. https://doi.org/10.1107/S1600536808041767
65. Müller C, Koch A, Görls H, Krieck S, Westerhausen M (2015) Tris(pyrazolyl)methanides of the Alkaline Earth Metals: Influence of the Substitution Pattern on Stability and Degradation. Inorg Chem 54:635–645. https://doi.org/10.1021/ic5025907
66. Claramunt RM, López C, Jaime C, Virgili A, Marco C, Elguero J (1995) The conformation of Trispyrazolylmethanes: an experimental and theoretical study. Heterocycles 40:175–186. https://doi.org/10.3987/COM-94-S6
67. Ochando LE, Rius J, Louër D, Claramunt RM, López C, Elguero J, Amigó JM (1997) Phase transitions in Tris(3,5-dimethylpyrazol-1-yl)methane. The structure of the high-temperature phase from X-ray powder diffraction. Acta Crystallogr B 53:939–944. https://doi.org/10.1107/S0108768197007830
68. Molčanov K, Milašinović V, Kojić-Prodić B (2019) Contribution of different crystal packing forces in π-stacking: from noncovalent to covalent multicentric bonding. Cryst Growth Des 19:5967–5980. https://doi.org/10.1021/acs.cgd.9b00540
69. Mooibroek TJ, Gamez P (2012) How directional are D-H···phenyl interactions in the solid state (D = C, N, O)? CrystEngComm 14:8462–8467. https://doi.org/10.1039/C2CE26205C
70. Cabrera AR, Gonzalez IA, Cortés-Arriagada D, Natali M, Berke H, Daniliuc CG, Camarada MB, Toro-Labbé A, Rojasa RS, Salasa CO (2016) Synthesis of new phosphorescent imidoyl-indazol and phosphine mixed ligand Cu(I) complexes——structural characterization and photophysical properties. RCS Adv 6:5141–5153. https://doi.org/10.1039/C5RA20450J
71. Kubiček K, Veedu ST, Storozhuk D, Kia R, Techert S (2017) Geometric and electronic properties in a series of phosphorescent heteroleptic Cu(I) complexes: Crystallographic and computational studies. Polyhedron 124:166–176. https://doi.org/10.1016/j.poly.2016.12.035
72. Bizzarri C, Fléchon C, Fenwick O, Cacialli F, Polo F, Gálvez-López MD, Yang CH, Scintilla S, Sun Y, Fröhlich R, De Cola L (2016) Luminescent neutral Cu(I) complexes: synthesis, characterization and application in solution-processed OLED. ECS J Solid State Sci Technol 5:R83–R90. https://doi.org/10.1149/2.0021606jss
73. Kitai A (2008) Luminescent materials and applications. Wiley, Chichester
74. Ghassemlooy Z, Alves LN, Zvánovec S, Khalighi MA (2017) Visible light communications: theory and applications. CRC Press, Boca Raton